

## Effect of melatonin loaded chitosan hydrogel on rat spinal cord injury

Fariborz Afroozi<sup>1</sup>, Ahmad Asghari<sup>1\*</sup>, Gholamreza Abedi<sup>1</sup>, Pejman Mortazavi<sup>2</sup>, Hesam Uddin Hoseinzadeh<sup>3</sup>

<sup>1</sup> Department of Veterinary Clinical Sciences, SR.C, Islamic Azad University, Tehran, Iran; <sup>2</sup> Department of Veterinary Pathobiology, SR.C, Islamic Azad University, Tehran, Iran; <sup>3</sup> Department of Veterinary Clinical Science, Ka.C, Islamic Azad University, Karaj, Iran.

### Article Info

#### Article history:

Received: 15 October 2024

Accepted: 01 February 2025

Available online: 15 September 2025

#### Keywords:

Chitosan

Melatonin

Rat

Spinal cord injury

### Abstract

Spinal cord injury (SCI) results in the demise of neural and glial cells, as well as extensive neuro- inflammation. Hydrogel formulation for prolonged release of melatonin (Mel) has demonstrated enhanced effectiveness and safety. In this study, SCI was induced in rats by contusion at the T<sub>9</sub> vertebrae. Chitosan (CH) /Mel hydrogel was fabricated and characterized using scanning electron microscopy (SEM) and Fourier transform infra-red to examine its specific effects on the apoptotic and histopathological markers of SCI. The scanning electron microscopy images revealed the presence of porosity in the CH/Mel hydrogel. Forty male Wistar rats were randomly divided into five groups (n = 8), including sham, control (SCI-induced treated locally with 100 µL CH hydrogel), and groups 3, 4, and 5 (treated locally immediately after SCI induction with 100 µL CH hydrogel containing 50.00, 100, and 200 mg kg<sup>-1</sup> Mel, respectively). The CH/Mel hydrogel at a dose of 25.00 mg mL<sup>-1</sup> significantly increased cell viability in the U87 cell line after 24 hr of exposure. However, at 48 and 72 hr after exposure, Bax and Bcl2 expressions were significantly increased and reduced in the SCI group, respectively, and CH/Mel hydrogel could alleviate their expressions, especially in higher doses. In addition, S100 protein expression was up-regulated in the SCI group. However, CH/Mel hydrogel down-regulated it in a dose-dependent manner. The histopathological findings demonstrated that CH/Mel hydrogel dramatically improved SCI outcomes, like vacuolar degeneration, necrosis, and severe cystic and axonal degenerations. In conclusion, CH/Mel hydrogel induced neuroprotection and it had the potential to be used as a therapeutic agent for the treatment of SCI.

© 2025 Urmia University. All rights reserved.

### Introduction

A highly relevant and socially significant matter in modern regenerative medicine is the restoration of spinal cord function in structural abnormalities of different origins predominantly resulting from traumatic damage.<sup>1</sup> Traumatic spinal cord injury (SCI) is a major contributor to disability. The SCI global incidence varies from 10.40 to 83.00 cases *per* million individuals annually, and is linked to lifetime healthcare costs ranging between 1.10 and 5.40 million USD in addition to incalculable societal and community costs.<sup>2</sup>

After SCI, complex molecular and chemical signaling pathways are triggered, leading to cell loss and tissue damage.<sup>3</sup> The primary insult in SCI arises from a mechanical trauma that directly affects the spinal cord and is followed by secondary phase reactions, including

inflammatory responses, ischemia, vascular malfunction, reactive oxygen species (ROS) generation, disrupted neural regulation, and cell death. This phase has a prominent role in impeding the restoration of spinal cord functioning.<sup>3,4</sup>

The occurrence of oxidative stress resulting from producing free radicals and lipid peroxidation is a characteristic feature of the secondary damage produced by SCI.<sup>5</sup> Significant emphasis has been on the oxidative stress cascade that occurs after SCI and leads to secondary damage. This is because it is believed that blocking the harmful effects of oxidative stress is a key strategy for therapeutic approaches.<sup>6</sup> Pro-inflammatory cytokines, including interleukin 1 $\alpha$  and  $\beta$ , are activated and released after SCI, and play a major role in immune and vascular responses. Tumor necrosis factor  $\alpha$  and interleukin -6 both play important roles in the pathogenesis of pro-

#### \*Correspondence:

Ahmad Asghari. DVM, DVSc

Department of Veterinary Clinical Sciences, SR.C, Islamic Azad University, Tehran, Iran

E-mail: dr.ahmad.asghari@srbiau.ac.ir



This work is licensed under a Creative Commons Attribution-NonCommercial-ShareAlike 4.0 International (CC BY-NC-SA 4.0) which allows users to read, copy, distribute and make derivative works for non-commercial purposes from the material, as long as the author of the original work is cited properly.

inflammatory damage following SCI.<sup>7,8</sup> It has been demonstrated that activation of the nuclear factor kappa  $\beta$  signaling pathway is critical for the induction of inflammation, and also contributes to the production of ROS and prostaglandins which work in concert to magnify the effects of inflammation.<sup>9</sup>

Treating SCI is difficult due to the intricate pathophysiological reactions and limited treatment opportunities. The present therapeutic options consist of two categories, including safeguarding the nerve cells and enhancing their regeneration.<sup>10</sup> The nerve cell protection is mostly utilized to prevent secondary damage, and has a proactive function in the initial stages following an injury. On the other hand, the second choice is employed to repair and regenerate nerve tissue to restore function and is commonly used during the afterward, chronic phase.<sup>11</sup>

Hydrogels are intricate structures made up of hydrophilic polymers that contain a significant quantity of water. Hydrogels have emerged as a promising biomaterial for various applications due to their adjustable physicochemical properties and less invasive nature.<sup>12</sup> Moreover, hydrogels minimize glial scar development and transport therapeutic drugs, cells, and other functional elements to mend and connect the spinal cord.<sup>13</sup> The appeal of natural hydrogels, like chitosan (CH), lies in their eco-friendly characteristics, biodegradability, cost-effective manufacturing, and ample availability of raw materials.<sup>14</sup>

Chitosan is a natural-based co-polymer that is positively charged and composed of N-acetyl-d-glucosamine and d-glucosamine units that are formed by the deacetylation of chitin. It possesses remarkable biological characteristics, such as non-toxicity and biocompatibility. Due to these characteristics, CH and its derivatives are frequently utilized in biomedical in the form of nanoparticles, fibers, films, and hydrogels.<sup>15,16</sup>

Melatonin (Mel; N-acetyl-5-methoxytryptamine) is primarily produced and released by the pineal gland *via* hydroxylation of tryptophan; however, it is also generated in very small quantities by the retina, hardierian gland, gastrointestinal system, and lymphocytes.<sup>5</sup> Melatonin has different neuroprotective properties, such as anti-oxidant and anti-inflammatory effects.<sup>17</sup> In addition to activating multiple anti-oxidant enzymes, Mel can scavenge a range of ROS and reactive nitrogen species.<sup>17,18</sup>

This study was aimed to evaluate the impact of Mel loaded CH (CH/Mel) hydrogel on SCI in an animal model.

## Materials and Methods

**Fabrication of CH/Mel hydrogel.** The CH solution was prepared by dissolving medium molecular weight CH from crab shells (~400 kDa and 85.00% deacetylated; Fluka, Sigma-Aldrich, St. Louis, USA) in a 1.00% aqueous solution (v/v) of glacial acetic acid (Merck, Darmstadt,

Germany) to a concentration of 2.00% (w/v) with stirring on a magnetic stirrer hot plate. The solution was stirred for 3 hr at low heat (50.00 °C). The resulting CH solution was filtered through a Whatman No. 3 filter paper and then, vacuum filtered to remove undissolved particles. To overcome the fragility of CH, glycerol (Sigma-Aldrich) was added at 30.00% (w/w) of the total weight of solid in the solution. Melatonin was purchased from Sigma-Aldrich. It was dissolved in ethanol and then, mixed with the CH solution. The resulting mixture was placed into 24-well plates, frozen, and lyophilized at - 80.00 °C for 48 hr. Solutions were prepared to achieve a ratio of 1/100 (w/w) for Mel and CH, respectively.<sup>19,20</sup>

**Electrostatic interactions determination.** Using Fourier transform infra-red (Nexus Analytics, Petaling Jaya, Malaysia) spectroscopy, the electrostatic interactions between CH and Mel in a formulation were tested. An average of 32 scans in the wave range between 400  $\text{cm}^{-1}$  and 4,000  $\text{cm}^{-1}$  with a resolution of 4.00  $\text{cm}^{-1}$  yielded FTIR spectra from test samples were used.

**Morphological study.** Scanning electron microscopy (KYKY-2800B SEMKYKY Technology Co., Ltd., Beijing, China) with electron acceleration voltage of 20.00 kilovolts was utilized to examine the structure of the created hydrogels. The specimens were treated through sputter coating where a tiny layer of gold was applied using an automated sputter fine coater. Subsequently, test samples were subjected to scanning electron microscope (SEM) to get images.

**Induction of SCI and grouping.** Male Wister rats (250 -280 g) were utilized in this study, and the animal procedures were performed completely in accordance with the guidelines of the Ethics Committee of the Islamic Azad University, Tehran, Iran (Ethics Code: IR.IAU.SRB.REC.1402.0216). Animals were randomly divided into five groups (n = 8), including sham, control (SCI-induced treated locally with 100  $\mu\text{L}$  CH hydrogel), and groups 3, 4, and 5 (treated locally immediately after SCI induction with 100  $\mu\text{L}$  CH hydrogel containing 50.00, 100, and 200  $\text{mg kg}^{-1}$  Mel, respectively). The dosage was chosen based on a work by others that evaluated neuroprotective effects of Mel on experimental SCI in rats.<sup>21</sup> Before the procedure, the animals were first anesthetized with a combination of xylazine (5.00  $\text{mg kg}^{-1}$ ; Alfasan, Woerden, Netherlands) and ketamine (80.00  $\text{mg kg}^{-1}$ ; Alfasan) intraperitoneally. A New York University impactor apparatus (Precision Systems & Instrumentation, Lexington, USA) was then utilized to create the appropriate contusive pressure. The rats were positioned in a prone position and immobilized at the T<sub>8</sub> and T<sub>10</sub> vertebrae using the clips of the impactor. Upon accurately identifying the 9<sup>th</sup> thoracic vertebra, a larger portion of the skin above it was shaved and cleaned. The epidermis and connective tissue were further detached with blunt instruments, and the lamina of the T<sub>9</sub> vertebra was carefully removed with a dental drill to

expose the spinal cord. A 10.00 g weight was then dropped from a height of 25.00 cm on the exposed portion of the spinal cord to cause the contusion. The presence of flutter reflexes in the tail and sudden retraction of the hind limbs were considered indicative of successful implementation of the model.<sup>21</sup>

#### Histopathology and immunohistochemistry (IHC).

For this purpose, the animals were anesthetized using ketamine 80.00 mg kg<sup>-1</sup> and xylazine 10.00 mg kg<sup>-1</sup> intraperitoneally. Then, the animals were transcardially perfused with a fixative containing 2.00% paraformaldehyde and 1.00% glutaraldehyde buffer (pH: 7.40) and their whole spinal cords were removed for subsequent study. The dissected spinal cord at the damage location was subsequently split into two distinct segments. One segment was preserved at RNAlater solution for quantitative real-time polymerase chain reaction (qRT-PCR), while the other segment was immersed in 10.00% formaldehyde for 48 hr to facilitate histological analyses. After fixation, the samples were immersed in paraffin for embedding. Subsequently, sections of 5.00 mm in thickness were produced both transversely and longitudinally and utilized for either Hematoxylin and Eosin staining or IHC. Finally, an experienced pathologist examined and evaluated the slides thoroughly with a light microscope (Olympus BX51, Tokyo, Japan) and documented all changes detected in a blank form. The evaluations were qualitative based on the work of others.<sup>22</sup> The sections for IHC were stained with a rabbit polyclonal antibody against S100 (dilution of 1:400; Dako, Santa Clara, USA).<sup>21</sup>

**Apoptosis related genes (*Bax* and *Bcl2*) expression quantification by qRT-PCR.** For this purpose, the animals were anesthetized using ketamine 80.00 mg kg<sup>-1</sup> and xylazine 10.00 mg kg<sup>-1</sup> intra-peritoneally. Spinal cord samples were subjected to the total RNA extraction using Trizol reagent (Biobasic, Markham, Canada), followed by cDNA synthesis using the cDNA synthesis kit (Zistvirayesh, Tehran, Iran). The qRT-PCR was conducted in triplicate using SYBR Green Master Mix (Zistvirayesh) on StepOne-Plus apparatus (Applied Biosystems, Waltham, USA). The relative expression levels of *Bax* and *Bcl2* were calculated using the  $\Delta\Delta C_t$  method, with  $\beta$ -actin serving as a house-keeping gene and the following primers:  $\beta$ -actin (forward) 5'CAACCTTCTTGCAGCTCCTC3',  $\beta$ -actin (reverse) 5' TTCTGACCCATACCCACCAT3', *Bax* (forward) 5' GCCTCCTTTCCTACTTCGGG3', *Bax* (reverse) 5'CTTTCCCCGTTCCCCATTCA3', *Bcl2* (forward) 5' TCGCGACTTTCAGAGATGT3', and *Bcl2* (reverse) 5' CAATCCTCCCCAGTTC ACC 3'. After sampling, the animals were euthanized using intra-peritoneal overdose of 400 mg kg<sup>-1</sup> ketamine and 40.00 mg kg<sup>-1</sup> xylazine.

**Statistical analysis.** Statistical analyses were performed using SPSS Software (version 24.0; IBM Corp., Armonk, USA). First, the normal distribution of the data

was checked using the Kolmogorov-Smirnov test (a non-parametric statistical test). Every *in vitro* experiment was run in triplicate and statistical analysis was performed using the mean data. One-way analysis of variance was used to see whether any significant differences existed and followed by the Tukey *post-hoc* test to ascertain the group differences. The *p* values were regarded as statistically significant if they were less than 0.05.

## Results

**Characterization of CH/Mel hydrogel.** Chitosan was identified through various absorption bands in the FTIR spectrum (Fig. 1). The presence of hydroxyl (-OH) groups and free amino (-NH<sub>2</sub>) was respectively confirmed at 3,439 cm<sup>-1</sup> and 1,160 cm<sup>-1</sup>, indicating the existence of CH. A broad band, ranging from 3,400 to 2,500 cm<sup>-1</sup>, corresponds to the stretching of C-H bonds. Additionally, absorption bands at around 2,872 cm<sup>-1</sup> signify C-H asymmetric stretching. The presence of residual N-acetyl groups was confirmed by bands at approximately 1,658 cm<sup>-1</sup> (C=O stretching of amide I) and 1,323 cm<sup>-1</sup> (C-N stretching of amide III). Moreover, a strong absorption region between 1,200 - 800 cm<sup>-1</sup> indicated the presence of polysaccharide skeleton, including the vibration of the glycoside bonds, as well as C-O and C-O-C stretching. Furthermore, in the FTIR spectrum of CH, the characteristic peaks at 1,020 and 1,150 cm<sup>-1</sup> corresponded to the C-O bonding and asymmetric extension of the C-O-C bridge, respectively. In the FTIR spectrum, Mel exhibited specific peaks, indicating its molecular structure. It showed a sharp peak at 3,325 cm<sup>-1</sup> for N-H bending and a peak at 3,160 cm<sup>-1</sup> for C-N stretching. Additionally, peaks were observed at 1439 and 1,563 cm<sup>-1</sup> for aromatic C = and at 1611 cm<sup>-1</sup> for C=O. The FTIR analysis of CH nanoparticles (CSNPs) revealed a broadened -OH stretching peak around 3,400 cm<sup>-1</sup>, likely indicating the formation of nanoparticles. Furthermore, differences observed between the Mel-CSNPs and CSNPs spectra suggested complete encapsulation of Mel, as indicated by the FTIR analysis.

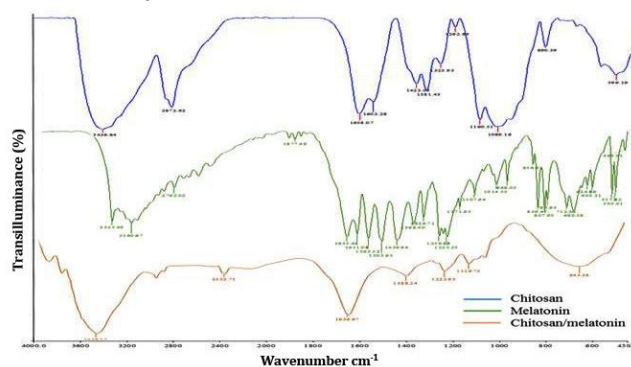


**Fig. 1.** The Fourier transform infra-red (FTIR) spectra of the melatonin, chitosan, and CH/Mel hydrogel.

The SEM was used to analyze the morphology of cross-section of the freeze-dried CH/Mel hydrogel. The SEM demonstrated that the freeze-dried CH/Mel hydrogel had a porous and inter-connected pore structure (Fig. 2). This particular shape was well-suited for the transfer of nutrients and metabolites. Therefore, CH/Mel hydrogel offered a suitable framework for cellular adhesion and growth.

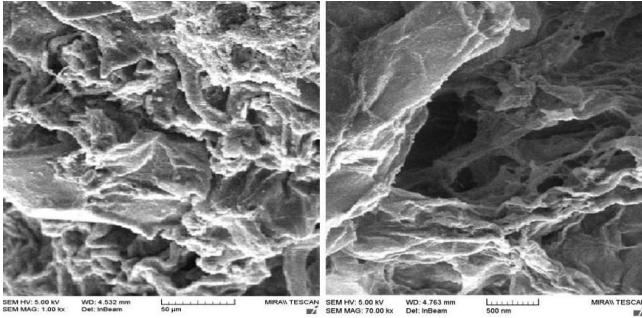


**Fig. 2.** The scanning electron microscope (SEM) micrograph of CH/Mel hydrogel at different magnifications.

**Apoptosis related genes expression pattern after SCI.** Based on the data shown in Figure 3, the expression level of the *Bax* gene in the control group was found to be 1.85 times higher than that of the sham group. Also, the CH/Mel hydrogel demonstrated a dose-dependent reduction in *Bax* gene expression compared to the control group. Furthermore, the expression of the *Bcl2* gene which acts as an anti-apoptotic gene was dropped by a factor of 2.60 in the control group compared to the sham group that recovered with the use of CH/Mel hydrogel (Fig. 3).

**Histopathology and IHC.** Histopathological analyses were carried out 30 days after SCI at T<sub>9</sub> segment. Hematoxylin and Eosin staining indicated that in the SCI group inflammatory cell infiltrations, vacuolar degenerations, and severe cystic and axonal degenerations in the anterior funicular region were observed.

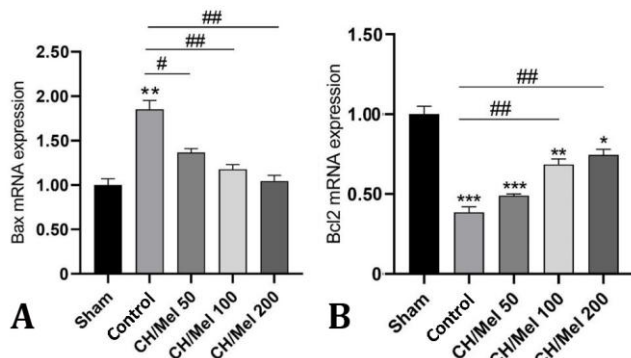


**Fig. 3.** Gene's expression of A) *Bax* and B) *Bcl2* following chitosan/melatonin (CH/Mel) hydrogel treatment in a rat model of spinal cord injury. The values are presented as mean  $\pm$  standard error of three independent experiments ( $n = 3$ ; each measured in duplicate). \*, \*\*  $p < 0.01$  and \*\*\*  $p < 0.001$  vs. control group. #  $p < 0.05$  vs. sham and Ch/Me200 groups. ##  $p < 0.05$  vs. sham group.

Additionally, the boundaries between gray and white matter in the spinal cord were unclear. In addition, significant neuronal necrosis in the posterior horn occurred in this group (Figs. 4A and 4B).

Use of the CH/Mel hydrogel reduced gliosis and severe cystic and axonal degenerations in the injured spinal cord site; however, this reduction was clear in high doses of CH/Mel hydrogel. The necrotic nerve and inflammatory cells number in the group received 200 mg kg<sup>-1</sup> Mel were noticeably decreased in comparison with the SCI group (Figs. 4C - 4H).

The S-100 $\beta$  is a calcium-binding protein that mostly localized in astroglia and Schwann cells. The IHC results showed that the number of Schwann cells was noticeably higher in the Mel-treated groups in comparison with the control group (Figs. 4I - 4L).

## Discussion

In the present study, the results of *Bax* and *Bcl2* genes expression, as well as histopathological and IHC results showed that CH/Mel hydrogel could markedly ameliorate SCI damage. The SCI is a debilitating condition that primarily affects the central nervous system (CNS). It is typically the result of external trauma. Patients will experience permanent motor and sensory impairments as a consequence of neuronal loss and axonal disruption.<sup>23</sup> Current SCI therapeutic options include surgical decompression and stabilization, and use of vasopressor drugs and corticosteroids.<sup>24</sup> Nevertheless, both interventions are unable to fully resolve the issue of nerve regeneration at its core. The CH hydrogel with distinct benefits, like biocompatibility, mechanical strength, appropriate degradation rate, proper pore size, and high surface area, has the ability to surpass the constraints of surgical, drug, and cell therapies; hence, introducing novel possibilities for the SCI treatment.<sup>22-25</sup>

Pre-clinical research indicates that Mel has the potential to provide neuroprotective benefits and facilitate the recovery of neurological function following SCI. Various mechanisms, such as anti-oxidant properties, pro-inflammatory cytokines suppression, and apoptosis and autophagy inhibition may be implicated.<sup>17</sup>

Based on the FTIR analysis, CH effectively interacted with Mel. The SEM images revealed the presence of porosity in the CH/Mel hydrogel. These features were thought to enhance the ability of Mel to reduce the SCI secondary injury, like oxidative stress, inflammation, and apoptosis. The impaired micro-environment after SCI triggers secondary damages, such as neuro-inflammation and cellular apoptosis.<sup>26</sup> Melatonin through phosphoinositide 3-kinase /protein kinase B/ mammalian target of rapamycin signaling pathway and inhibition of mitochondrial dysfunction has improved SCI repair process in rats *via* enhanced autophagy and apoptosis

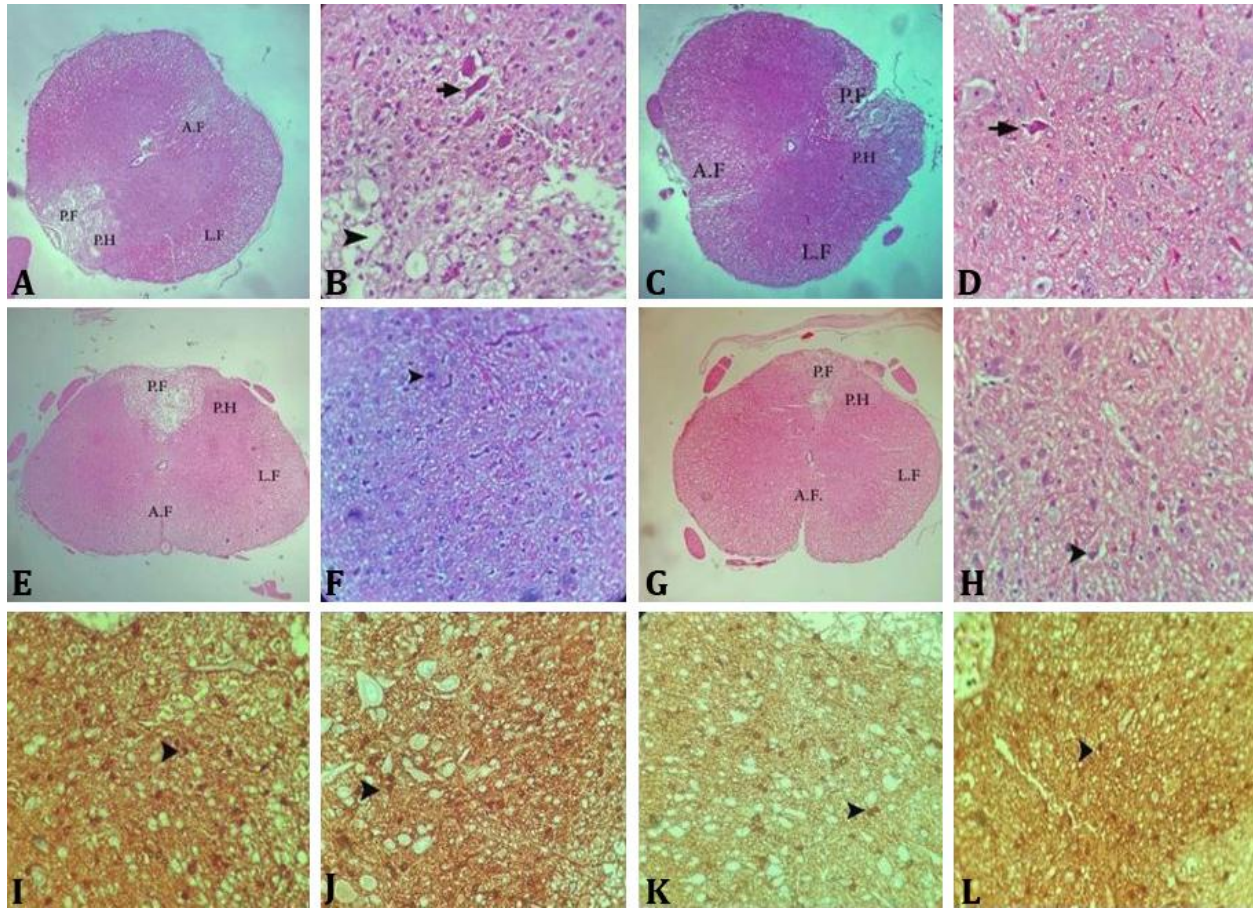


**Fig. 4.** Histopathological and immunohistochemical micrographs of the rats injured spinal cords in different experimental groups after four weeks injury. **A and B)** Control group; **C and D)** Chitosan/melatonin 50.00 mg kg<sup>-1</sup> group; **E and F)** Chitosan/melatonin 100 mg kg<sup>-1</sup> group; **G and H)** Chitosan/melatonin 200 mg kg<sup>-1</sup> group (Hematoxylin and Eosin staining; magnification in A, C, E, G = 20×, and in B, D, F, H = 400×). Arrow and arrowheads in B show pyknotic cells and axonal degeneration, respectively. Arrow in D shows necrotic neurons. Arrowhead in F shows shrunken cells with moderate pyknosis. Arrowhead in H shows slight shrinkage of the neuron. P.F: Posterior funiculus; L.F: Lateral funiculus; P.H: Posterior horn; A.F: Anterior funiculus. **I)** Control group; **J)** Chitosan/melatonin 50.00 mg kg<sup>-1</sup> group; **K)** Chitosan/melatonin 100 mg kg<sup>-1</sup> group; **L)** Chitosan/melatonin 200 mg kg<sup>-1</sup> group (immunohistochemical staining for S100β protein; magnification in I, J, K and L = 400×). Arrowheads in I, J, K and L show extensive, moderate, low and very mild damage to astrocytes, respectively.

inhibition.<sup>27,28</sup> In next step, the effects of different concentrations of Mel in CH/Mel hydrogel on *Bax* and *Bcl2* genes expression in a SCI model were analyzed. The *Bax* expression significantly increased in control group, and CH/Mel hydrogel could alleviate this expression, especially in higher doses; however, there was no difference between 100 and 200 mg kg<sup>-1</sup> of Mel. In addition, *Bcl2* gene expression as an anti-apoptotic gene significantly reduced in control group that recovered using CH/Mel hydrogel in three different doses. The recovery was significantly increased in the group treated with 200 mg kg<sup>-1</sup> Mel. Samantaray *et al.* have reported therapeutic potential of Mel in traumatic CNS injury.<sup>29</sup> Cayli *et al.* have studied the effect of combined treatment with Mel and methylprednisolone on neurological recovery after experimental SCI and concluded that Mel and Mel combined treatment modalities improve functional recovery at the same level.<sup>30</sup>

In other research, it was demonstrated that Mel had neuroprotective role in the injured part of CNS after SCI.<sup>5</sup> Hong *et al.* have suggested that the Mel combined with exercise would be a novel neuro-rehabilitative strategy for the faster recovery after SCI.<sup>31</sup>

Shen *et al.* have indicated that Mel effectively suppresses the expression of cleaved caspase-3 and *Bax*, while the expression of the anti-apoptotic protein *Bcl-2* is increased.<sup>32</sup> In another study, the combination of poly (lactic-co-glycolic acid)/sustained-release micro-spheres loaded Mel and Laponite hydrogel in the Lap/MS@Mel system effectively enhanced and extended the delivery of Mel to the injured spinal cord through *in situ* injection *in vivo*, and improved inflammation and apoptosis.<sup>33</sup>

The S100 protein family comprises versatile proteins that play a crucial role in governing various cellular processes. The S100β as a calcium-binding protein is

primarily produced by astrocytes in the CNS. Increased expression of S100  $\beta$ , along with glial fibrillary acidic protein, in the blood and cerebrospinal fluid is a typical sign of reactive astrogliosis.<sup>34</sup> In SCI models, S100 $\beta$  level in both serum and cerebrospinal fluid noticeably increases in a time-dependent manner.<sup>34</sup> Our IHC results showed that S100 protein expression was up-regulated in the control group and its expression was down-regulated in the CH/Mel hydrogel groups dose dependently.

Lorente *et al.* have hypothesized that non-survivor traumatic brain injury patients exhibit elevated ROS production compared to the survivor patients. Also, the elevated serum levels of total anti-oxidant capacity and Mel observed in these patients were an adaptive response aimed at restoring the balance between oxidant and anti-oxidant states in the face of heightened oxidant production. However, in individuals who did not survive, the rise in serum levels of total anti-oxidant capacity and Mel was insufficient to counterbalance the excessive production of ROS. As a result, these individuals experienced elevated peroxidation of protein, lipid, carbohydrate, and nucleic acid, which contributed to the cellular dysfunction and development of vasogenic edema.<sup>35</sup> Our histopathological findings demonstrated that CH/Mel hydrogel dramatically improved SCI outcomes, like vacuolar degeneration, necrosis, and severe cystic and axonal degenerations. Consistent with our findings, Esposito *et al.* have reported that Mel ameliorates traumatic experimental SCI in rats.<sup>36</sup> Bi *et al.*, consistent with the findings of the present study, have suggested that Mel can effectively ameliorate SCI by inhibiting neuronal apoptosis and promoting neuronal repair.<sup>37</sup>

In conclusion, according to the findings of this study, it was proposed that CH/Mel hydrogel-induced neuro-protection was due to the suppression of apoptosis and S100 $\beta$ , which was associated with cell death, as well as inflammatory responses reduction, which were also heightened in SCI. However, the current study indicated that CH/Mel hydrogel had the potential to be used as a therapeutic agent for the treatment of SCI.

### Acknowledgments

This work was supported in part by the Vice-Chancellor for Research and Technology of Islamic Azad University, Science and Research Branch, Tehran, Iran, being acknowledged by the authors. This work was performed as a dissertation of first author submitted as a Partial Fulfillment of the Degree of Doctor of Veterinary Science in Veterinary Surgery at the Islamic Azad University, Science and Research Branch, Tehran, Iran.

### Conflict of interest

There are no conflicts of interests to be declared.

### References

1. Freyermuth-Trujillo X, Segura-Urbe JJ, Salgado-Ceballos H, et al. Inflammation: a target for treatment in spinal cord injury. *Cells* 2022; 11(17): 2692. doi: 10.3390/cells11172692.
2. Eli I, Lerner DP, Ghogawala Z. Acute traumatic spinal cord injury. *Neurol Clin* 2021; 39(2): 471-488.
3. Hachem LD, Fehlings MG. Pathophysiology of spinal cord injury. *Neurosurg Clin N Am* 2021; 32(3): 305-313.
4. Patek M, Stewart M. Spinal cord injury. *Anaesth Intensive Care* 2020; 21(8): 411-416.
5. Naseem M, Parvez S. Role of melatonin in traumatic brain injury and spinal cord injury. *Sci World J* 2014; 2014: 586270. doi: 10.1155/2014/586270.
6. Cristante AF, Barros Filho TE, Marcon RM, et al. Therapeutic approaches for spinal cord injury. *Clinics (Sao Paulo)* 2012; 67(10): 1219-1224.
7. Mao L, Wang H, Qiao L, et al. Disruption of Nrf2 enhances the upregulation of nuclear factor-kappaB activity, tumor necrosis factor- $\alpha$  and matrix metalloproteinase-9 after spinal cord injury in mice. *Mediators Inflamm* 2010; 2010: 238321. doi: 10.1155/2010/238321.
8. Ritz MF, Hausmann ON. Effect of 17 $\beta$ -estradiol on functional outcome, release of cytokines, astrocyte reactivity and inflammatory spreading after spinal cord injury in male rats. *Brain Res* 2008; 1203: 177-188.
9. Paterniti I, Genovese T, Crisafulli C, et al. Treatment with green tea extract attenuates secondary inflammatory response in an experimental model of spinal cord trauma. *Naunyn Schmiedebergs Arch Pharmacol* 2009; 380(2): 179-192.
10. Wang H, Zhang H, Xie Z, et al. Injectable hydrogels for spinal cord injury repair. *Eng Regen* 2022; 3(4): 407-419
11. Lin PH, Dong Q, Chew SY. Injectable hydrogels in stroke and spinal cord injury treatment: a review on hydrogel materials, cell-matrix interactions and glial involvement. *Mater Adv* 2021; 2(1): 2561-2583.
12. Thirupathi K, Raorane CJ, Ramkumar V, et al. Update on chitosan-based hydrogels: preparation, characterization, and its antimicrobial and antibiofilm applications. *Gels* 2022; 9(1): 35. doi: 10.3390/gels9010035.
13. Pakulska MM, Ballios BG, Shoichet MS. Injectable hydrogels for central nervous system therapy. *Biomed Mater* 2012; 7(2): 024101. doi: 10.1088/1748-6041/7/2/024101.
14. Shariatnia Z, Jalali AM. Chitosan-based hydrogels: preparation, properties and applications. *Int J Biol Macromol* 2018; 115: 194-220.
15. Aranaz I, Alcántara AR, Civera MC, et al. Chitosan: an

- overview of its properties and applications. *Polymers (Basel)* 2021; 13(19): 3256. doi: 10.3390/polym13193256.
16. Ardean C, Davidescu CM, Nemeş NS, et al. Factors influencing the antibacterial activity of chitosan and chitosan modified by functionalization. *Int J Mol Sci* 2021; 22(14): 7449. doi: 10.3390/ijms22147449.
  17. Zhang Y, Zhang WX, Zhang YJ, et al. Melatonin for the treatment of spinal cord injury. *Neural Regen Res* 2018; 13(10):1685-1692.
  18. Xie L, Wu H, Huang X, et al. Melatonin, a natural antioxidant therapy in spinal cord injury. *Front Cell Dev Biol* 2023; 11: 1218553. doi: 10.3389/fcell.2023.1218553.
  19. Kaczmarek-Szczepańska B, Ostrowska J, Kozłowska J, et al. Evaluation of polymeric matrix loaded with melatonin for wound dressing. *Int J Mol Sci* 2021; 22(11): 5658. doi: 10.3390/ijms22115658.
  20. Valencia C, Valencia CH, Zuluaga F, et al. Synthesis and application of scaffolds of chitosan-graphene oxide by the freeze-drying method for tissue regeneration. *Molecules* 2018; 23(10): 2651. doi: 10.3390/molecules23102651.
  21. Gholami M, Gilanpour H, Sadeghinezhad J, et al. Facile fabrication of an erythropoietin-alginate/chitosan hydrogel and evaluation of its local therapeutic effects on spinal cord injury in rats. *DARU* 2021; 29(2): 255-265.
  22. Gül S, Celik SE, Kalayci M, et al. Dose-dependent neuroprotective effects of melatonin on experimental spinal cord injury in rats. *Surg Neurol* 2005; 64(4): 355-361.
  23. Cai M, Chen L, Wang T, et al. Hydrogel scaffolds in the treatment of spinal cord injury: a review. *Front Neurosci* 2023; 17: 1211066. doi: 10.3389/fnins.2023.1211066.
  24. Karsy M, Hawryluk G. Modern medical management of spinal cord injury. *Curr Neurol Neurosci Rep* 2019; 19(9): 65. doi: 10.1007/s11910-019-0984-1.
  25. Ashammakhi N, Kim HJ, Ehsanipour A, et al. Regenerative therapies for spinal cord injury. *Tissue Eng Part B Rev* 2019; 25(6): 471-491.
  26. Wang H, Wang H, Huang H, et al. Melatonin attenuates spinal cord injury in mice by activating the Nrf2/ARE signaling pathway to inhibit the NLRP3 inflammasome. *Cells* 2022; 11(18): 2809. doi: 10.3390/cells11182809.
  27. Li Y, Guo Y, Fan Y, et al. Melatonin enhances autophagy and reduces apoptosis to promote locomotor recovery in spinal cord injury via the PI3K/AKT/mTOR signaling pathway. *Neurochem Res* 2019; 44(8): 2007-2019.
  28. Zhong G, Yang Y, Feng D, et al. Melatonin protects injured spinal cord neurons from apoptosis by inhibiting mitochondrial damage via the SIRT1/Drp1 signaling pathway. *Neuroscience* 2023; 534: 54-65.
  29. Samantaray S, Das A, Thakore NP, et al. Therapeutic potential of melatonin in traumatic central nervous system injury. *J Pineal Res* 2009; 47(2): 134-142.
  30. Cayli SR, Kocak A, Yilmaz U, et al. Effect of combined treatment with melatonin and methylprednisolone on neurological recovery after experimental spinal cord injury. *Eur Spine J* 2004; 13(8): 724-732.
  31. Hong Y, Palaksha KJ, Park K, et al. Melatonin plus exercise-based neurorehabilitative therapy for spinal cord injury. *J Pineal Res* 2010; 49(3):201-209.
  32. Shen Z, Zhou Z, Gao S, et al. Melatonin inhibits neural cell apoptosis and promotes locomotor recovery via activation of the Wnt/ $\beta$ -catenin signaling pathway after spinal cord injury. *Neurochem Res* 2017; 42(8): 2336-2343.
  33. Zhang M, Bai Y, Xu C, et al. Novel optimized drug delivery systems for enhancing spinal cord injury repair in rats. *Drug Deliv* 2021; 28(1): 2548-2461.
  34. Duan K, Liu S, Yi Z, et al. S100- $\beta$  aggravates spinal cord injury via activation of M1 macrophage phenotype. *J Musculoskelet Neuronal Interact* 2021; 21(3): 401-412.
  35. Lorente L, Martín MM, Abreu-González P, et al. Serum melatonin levels in survivor and non-survivor patients with traumatic brain injury. *BMC Neurol* 2017; 17(1): 138. doi: 10.1186/s12883-017-0922-2.
  36. Esposito E, Genovese T, Caminiti R, et al. Melatonin regulates matrix metalloproteinases after traumatic experimental spinal cord injury. *J Pineal Res* 2008; 45(2): 149-156.
  37. Bi J, Shen J, Chen C, et al. Role of melatonin in the dynamics of acute spinal cord injury in rats. *J Cell Mol Med* 2021; 25(6): 2909-2917.